Resource

Chemistry & Biology

Profiling of Free Fatty Acids Using Stable Isotope Tagging Uncovers a Role for Saturated Fatty Acids in Neuroexocytosis

Graphical Abstract

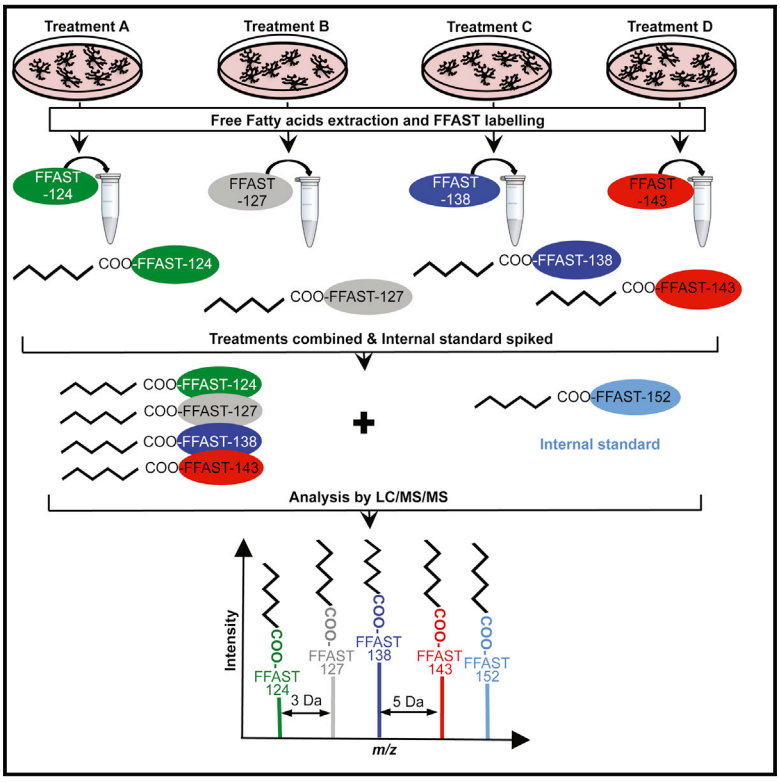

Highlights

- FFAST method enables multiplexed fatty acid profiling with nanomolar sensitivity
- Main free fatty acids (FFAs) generated during neuroexocytosis are saturated
- Generation of saturated FFAs suggests an unexpected role of PLA1
- FFAs generated in secretory vesicles highlights a key role for Ca^{2+} and cytosol

Authors

Vinod K. Narayana, Vanesa M. Tomatis, Tong Wang, David Kvaskoff, Frederic A. Meunier

Correspondence

f.meunier@uq.edu.au (F.A.M.), david.kvaskoff@bzh.uni-heidelberg.de (D.K.)

In Brief

Narayana et al. developed a free fatty acid stable isotope tagging (FFAST) method that enables multiplexed quantification of endogenous free fatty acids with nanomolar sensitivity. Here, they uncover an unexpected variety of change in free fatty acids generated during neuroexocytosis in neurons and chromaffin cells.

Narayana et al., 2015, Chemistry & Biology 22, 1552–1561
November 19, 2015
http://dx.doi.org/10.1016/j.chembiol.2015.09.010

CellPress

CellPress

Chemistry & Biology
Resource

Profiling of Free Fatty Acids Using Stable Isotope Tagging Uncovers a Role for Saturated Fatty Acids in Neuroexocytosis

Vinod K. Narayana,[1] Vanesa M. Tomatis,[1,2] Tong Wang,[1] David Kvaskoff,[1,3,*] and Frederic A. Meunier[1,*]
[1]Clem Jones Centre for Ageing Dementia Research, Queensland Brain Institute, The University of Queensland, QLD 4072, Australia
[2]Present address: Division of Cell Biology and Molecular Medicine, Institute for Molecular Bioscience, The University of Queensland, QLD 4072, Australia
[3]Present address: Heidelberg University Biochemistry Centre, Im Neuenheimer Feld 328, 69120 Heidelberg, Germany
*Correspondence: f.meunier@uq.edu.au (F.A.M.), david.kvaskoff@bzh.uni-heidelberg.de (D.K.)
http://dx.doi.org/10.1016/j.chembiol.2015.09.010

SUMMARY

The phospholipase-catalyzed release of free fatty acids (FFAs) from phospholipids is implicated in many critical biological processes such as neurotransmission, inflammation, and cancer. However, determining the individual change in FFAs generated during these processes has remained challenging due to the limitations of current methods, and has hampered our understanding of these key mediators. Here, we developed an "iTRAQ"-like method for profiling FFAs by stable isotope tagging (FFAST), based on the differential labeling of the carboxyl group and designed to resolve analytical variance, through a multiplexed assay in cells and subcellular fractions. With nanomolar sensitivity, this method revealed a spectrum of saturated FFAs elicited during stimulation of exocytosis that was identical in neurons and neurosecretory cells. Purified secretory vesicles also generated these FFAs when challenged with cytosol. Our multiplex method will be invaluable to assess the range of FFAs generated in other physiological and pathological settings.

INTRODUCTION

Fatty acids provide the two hydrophobic tails of glycerophospholipids, which are essential components of cellular membranes. Each of these lipids comprises a saturated and an unsaturated fatty acid chain. The critical role played by saturated fatty acids in conveying nanostructural organization of the plasma membrane via transbilayer interaction was recently revealed (Raghupathy et al., 2015). The length of the saturated chain is paramount in mediating these essential transbilayer effects (Raghupathy et al., 2015). Importantly, these phospholipids can be targeted by phospholipases to release one fatty acid moiety called a free fatty acid (FFA) to become a lysophospholipid (Kihara et al., 2014). This conversion occurs during physiological processes such as neuroexocytosis (Darios et al., 2007), long-term potentiation (Williams et al., 1989), and inflammation (Shimizu, 2009), and both FFAs and lysophospholipids have signaling as well as membrane curvature and fluidity effects (Rigoni et al., 2005). Arachidonic acid (AA) is one of such molecule that initiates a cascade of bioactive signaling molecules. Recent work has suggested that the specific combinations of FFAs and lysophospholipids have previously unsuspected effects in triggering neurotransmitter secretion (Rigoni et al., 2005). However, identifying and determining the global changes in concentrations of each endogenous FFA precisely has been a major hurdle to understanding their role individually and in combination with lysophospholipids at the cellular level. Moreover, a precise understanding of which specific FFA is generated could help to complete the picture of the actions of various phospholipases on membrane fluidity and generation of bioactive derivatives.

Clearly, establishing an unbiased method to unravel the absolute change in FFAs produced during important physiological processes, such as neuroexocytosis and inflammation, is needed. The detection of FFAs by mass spectrometry (MS) is arduous in their native form due to their high polarity, poor ionization of the carboxyl acid group (Hellmuth et al., 2012; Johnson, 2005; Kanawati and Schmitt-Kopplin, 2010), and the non-specific loss of either carbon dioxide or water (Johnson, 2005; Johnson and Trinh, 2003). The identification of FFAs is also easily affected by matrix effects, and sensitivity is low. As a result, most quantitative analyses are carried out by gas chromatography-MS of the fatty acid methyl esters (Moldovan et al., 2002; Seppanen-Laakso et al., 2002), but this technique is not amenable to multiplexing.

Recent studies have concentrated on derivatizing the carboxyl group of fatty acids in an attempt to solve these sensitivity and specificity issues (Leng et al., 2013; Li and Franke, 2011; Yang et al., 2007). However, although some of these new techniques have improved sensitivity issues, no integrative method has yet been designed to overcome issues related to biological and assay variability, which often lead to misinterpretation of the results. Moreover, these early methods have so far been limited to comparison of only two separate conditions (Koulman et al., 2009; Lamos et al., 2007). It is therefore of great importance to develop a more effective strategy that results in simultaneous quantitative and qualitative analysis of FFAs. By derivatizing FFA with a labeled pyridinium side chain and by modulating the extent of deuteration, we have now addressed these challenges. We describe a multiplexed FFA quantification strategy

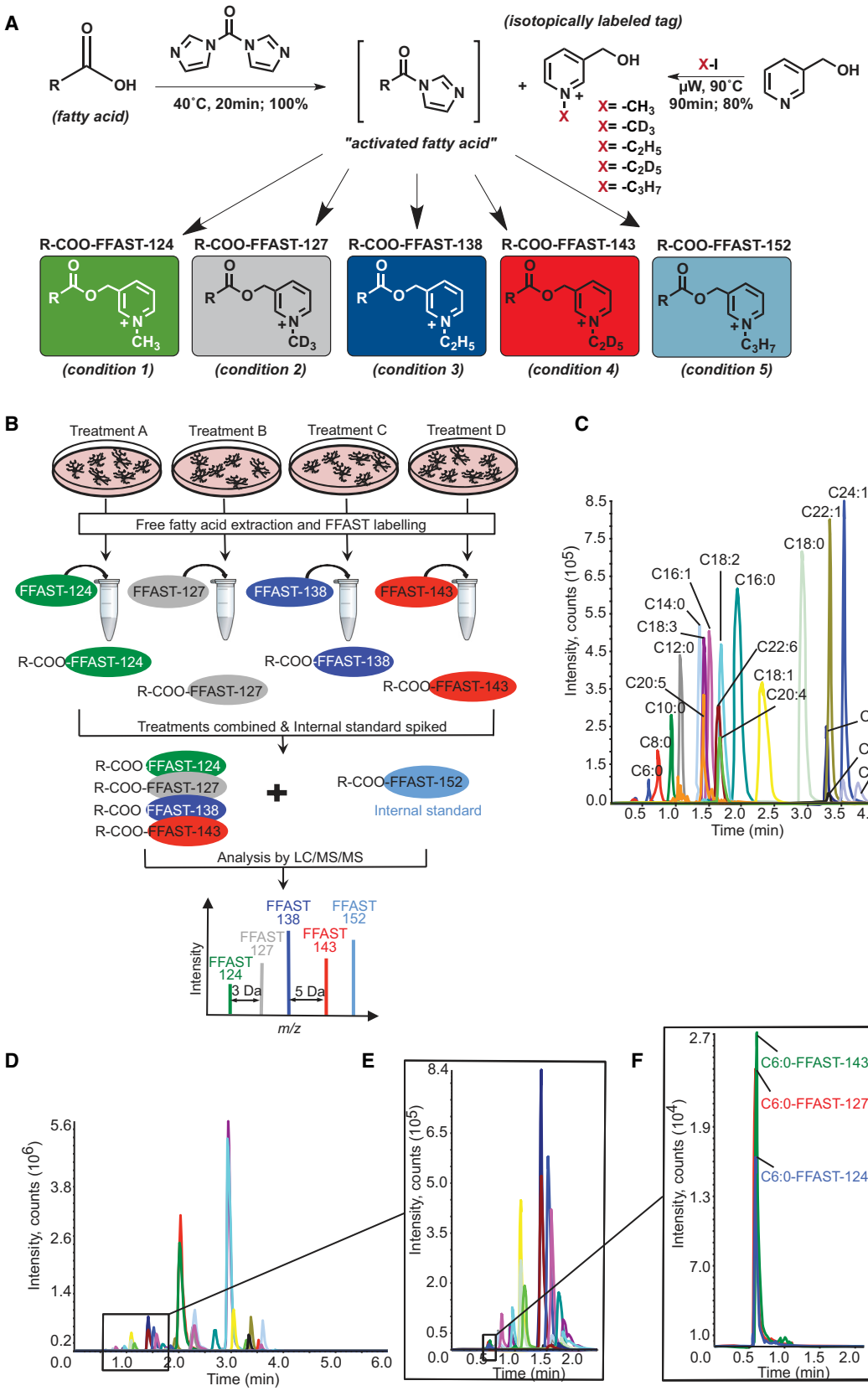

(legend on next page)

that provides direct comparisons of relative and absolute measurements of four samples in complex matrices with internal standards in one analytical run. This iTRAQ-like technique, which provides a 2,500-fold increase in sensitivity, allows the determination of an array of FFAs generated during stimulation of exocytosis in cultured cortical neurons and bovine chromaffin cells. We have uncovered a consistent pattern in the FFAs generated during stimulation in both models and in a subcellular fraction enriched in purified secretory vesicles (chromaffin granules). Our result underpins common, albeit unknown, mechanisms in both cell types leading to the production of mostly saturated FFAs, thereby challenging our current understanding of the involvement of phospholipases in exocytosis. Our FFAST method has led us to uncover a surprisingly high number of FFA changes during stimulation of exocytosis, revealing an unprecedented level of complexity in the underpinning molecular mechanisms.

RESULTS

Establishing an FFA Profiling Method

Derivatization of FFAs as picolinyl esters increases their detection sensitivity (Koulman et al., 2009; Yang et al., 2007). Although such derivatization has already been combined with the use of isotopes, this comparative approach has so far been limited to relative FFA measurements in only two sample conditions. We reasoned that the reactive nitrogen group of hydroxymethylpyridine could be used to incorporate isotopic tags of varying chain lengths with a view to designing a true multiplexed quantitative assay for FFAs. These tags can specifically react with the carboxyl group of the fatty acid in a straightforward, one-step derivatization reaction (Figure 1A).

We generated the following isotopic tags: 3-hydroxymethyl-1-methylpyridium iodide (FFAST-124), 3-hydroxymethyl-1-methyl-d_3-pyridium iodide (FFAST-127), 3-hydroxymethyl-1-ethylpyridium iodide (FFAST-138), 3-hydroxymethyl-1-ethyl-d_5-pyridium iodide (FFAST-143), and 3-hydroxymethyl-1-propylpyridium iodide (FFAST-152) of varying mass, *m/z* 124, 127, 138, 143, 152, respectively (Figure 1A). The hydroxyl group of the FFAST labels specifically reacts with the carboxyl group of FFAs pre-activated with 1,1-carbonyldiimidazole, leading to derivatized FFAs (Figure 1A). Four of the FFAST labels (FFAST-124, -127, -138, -143) were used to derivatize endogenous FFAs extracted with methyl-*tert*-butyl ether (MTBE) from cells exposed to four different conditions (Figure 1B). Derivatization of the endogenous FFAs with the FFAST tags offered mass changes such as 3 Da (between FFAST-124 and -127) and 5 Da (between FFAST-138 and -143) (Figure 1B). Following derivatization the samples were combined, and 19 internal standards were spiked to normalize the relative signal response between the endogenous and deuterated derivatives (Figure 1B). These FFAs, including saturated and unsaturated (6–24 carbons), were chosen as reference standards and derivatized in advance with the FFAST-152 tag (Figure 1A, condition 5). The combined sample was then analyzed by liquid chromatography-tandem MS (LC-MS/MS) and the result for each analyte was compared with its own reference standard (Figure 1B). This multiplexed strategy is similar to the well-established iTRAQ approach in proteomics (Wiese et al., 2007). The permanently charged ionizable group tagging the endogenous FFAs increases the ionization efficiency and, thus, the detection sensitivity, enhancing the signal response 2,500-fold (Figure 1C).

In preparation for the development of the LC-MS/MS assay, product ion-scanning experiments were conducted using collision gas. The introduction of the isotopic tag (basic group) or a permanently charged group on the FFAs increases the ionization efficiency, allowing their detection at nanomolar concentrations (Figure S3). The collision energy, declustering potential, and entrance potential were uniformly optimized to generate product ions at *m/z* 124 (FFAST-124), *m/z* 127 (FFAST-127), *m/z* 138 (FFAST-138), *m/z* 143 (FFAST-143), and *m/z* 92 and *m/z* 152 (FFAST-152) specific for each tag. This approach was used to specifically select the mass fragment pairs corresponding to the fatty acyl chain and its corresponding label (Table S1). As a result, a large number of FFAs could be monitored simultaneously and a complete baseline separation was not necessary (Figures 1 and 2). The ion pairs and corresponding chromatography retention times are presented in Figures 1D and Tables S2 and S3.

The aim of different isotopic tags is to precisely quantify the relative abundance of FFAs in multiplexed samples, independent of matrix effects and inter-assay variations. To achieve this, the signals of isotopically labeled FFAs were compared as a ratio (FFAST-124, FFAST-127, FFAST-127, and FFAST-138 to FFAST-152). As a result, every FFAST-152-labeled FFA acts as an internal standard reference. This compensates for ion suppression and matrix effects that would otherwise bias the results. This procedure is normally difficult to achieve with a high number of analytes, which requires an equal number of synthetic deuterated standards. We have carried out a complete validation for all the 19 FFAs used in this study using matrix-matched standards (spiked cell extracts). Quantification was performed using standard curves, constructed for each analyte over the range 0.3 to 300 nM. Calibration lines were calculated by the least-squares linear regression method of the peak area ratio (response factor); the correlation was 0.9 for both

Figure 1. Implementation of Free Fatty Acid Stable Isotope Tagging for the Sensitive Detection of FFAs in Different Conditions Simultaneously

(A) Synthesis of the isotopic tags and derivatization of endogenous FFA.

(B) Key steps in our FFAST method workflow.

(C) LC-MS/MS chromatogram of isotope-tagged FFA derivatives from standards (50 pg/ml per compound).

(D–F) Typical LC-MS/MS profile of FFAs extracted from rat cortical neurons after stimulation by depolarization and following FFAST derivatization. FFAs from unstimulated sample were derivatized with FFAST-124 label and stimulated sample with FFAST-127, samples being mixed and analyzed simultaneously. FFAs samples from each condition were mixed together and analyzed simultaneously against each respective FFA internal standard preliminarily derivatized with FFAST-143. The zoom ratio of inset spectra (E and F) shows an example of an extracted ion chromatogram of hexanoic acid from all the samples analyzed at the same time with its own internal reference standard.

See also Figures S1 and S2, Tables S1–S5.

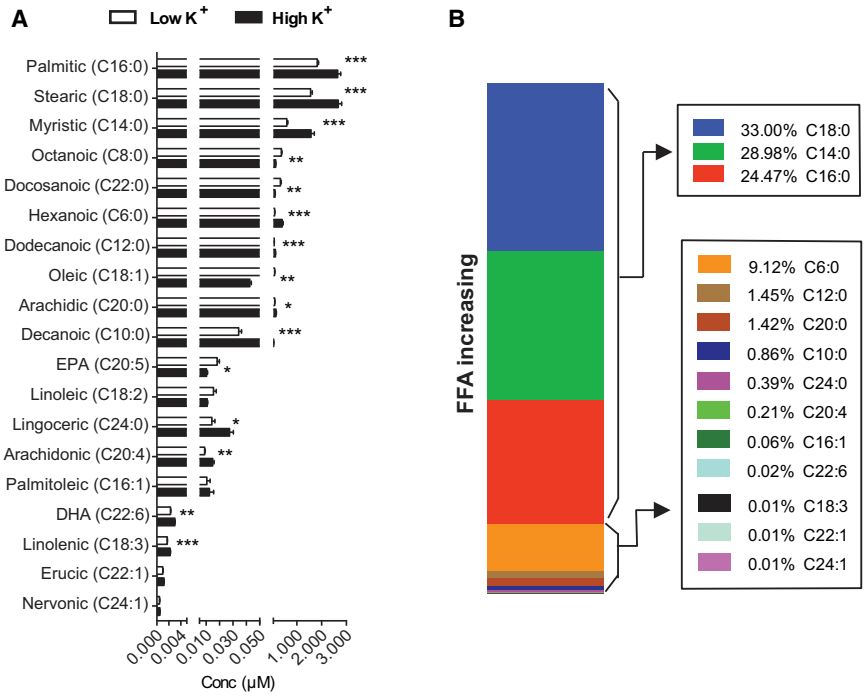

Figure 2. Quantification of FFA Changes in Stimulated Rat Cortical Neurons by FFAST Labeling

Rat cortical neurons (DIV21) were either stimulated for 15 min by depolarization or left unstimulated. Cells were then scrapped, lipids extracted, and FFAs derivatized as described in the Experimental Procedures.

(A) Changes in saturated and unsaturated FFAs elicited by stimulation.

(B) Stacked bar-graph representation of the FFAs increasing in concentration upon stimulation. The difference in concentration between unstimulated and stimulated was calculated, expressed as a percentage and stacked from the highest to the lowest. Note that the main FFAs produced in response to stimulation are saturated (stearic, palmitic, and myristic acids) and constitute 86.5% of the total FFAs generated.

Data are represented as mean ± SEM; *$p < 0.05$; **$p < 0.01$; ***$p < 0.001$, two-tailed Student's *t*-test.

saturated and unsaturated FFAs, showing that the assay was linear over this range of concentrations (Table S4). The lower limit of quantitation, defined as the lowest observable concentration with a minimum peak signal-to-noise ratio of 10, was on the order of 0.24 nM, corresponding to a sensitivity of approximately 1.2 fmol on column (5 μl injection volume) (Table S5). We estimated the imprecision (% coefficient of variation [CV]) and inaccuracy (% relative error) for a set of three matrix-matched quality controls at 1, 6, and 15 nM (quality control level 1, 2, and 3, respectively) (Table S5). The results remained within acceptable guidelines, i.e. mean CV <20% and mean accuracy within 80%–120% (U.S. Department of Health and Human Services et al., 2001, 2013). The freeze-thaw stability, intra- and inter-assay variations were estimated; mean imprecision and mean inaccuracy were both within 10% (Table S5).

The recovery of the extraction methodology was calculated after spiking chromaffin cells with a known amount of deuterium-labeled stearic acid-d_{35}. Following MTBE extraction, the endogenous and spiked FFAs were derivatized using the FFAST-124 label. The analysis of the peak area for extracted analytes was compared with the known amount of deuterium-labeled stearic acid-d_{35} standard, from which recovery was calculated to be 86% ± 5%.

Quantifying FFAs Following Stimulation in Cortical Neurons

FFAs are incorporated in lipids such as triglycerides, phospholipids, and cholesterol esters, and can be released by the action of phospholipase enzymes during physiological processes such as neuroexocytosis. In neurosecretory cells, AA is released from the *sn-2* position of phospholipids following cleavage by phospholipase-A2 (PLA2) activity (Latham et al., 2007; Morgan and Burgoyne, 1990; Ray et al., 1993; Rickman and Davletov, 2005). However, to date the actual concentration of AA produced has not been determined, nor is it known whether other FFAs are co-released during neuroexocytosis. Moreover, as AA is a key effector in long-term potentiation (Carta et al., 2014; Williams et al., 1989), determining how much AA is generated from neurons and comparing this with other FFAs is of great interest.

We therefore analyzed the changes in FFAs that occurred following stimulation of rat cortical neurons for 15 min in a depolarizing KCl buffer. Unstimulated neurons were used as a control, and the extracted endogenous FFAs were derivatized with the FFAST-124 label. The FFA extracts from the stimulated cells were derivatized with FFAST-127. A fixed amount of 19 FFA standards derivatized using FFAST-143 was added as the internal standard reference (Figures 1D–1F). The ratios of FFAs for each condition were measured against its own internal standard, and the variation of the ratios was plotted over the concentration (Figure 2A). Importantly 19 FFAs were identified, among which 10 in particular, saturated FFAs, showed a significant increase in concentration in response to secretagogue stimulation (Figure 2A). Indeed stearic, palmitic, and myristic acids represented 86% of the FFAs generated (Figure 2B). Although AA was indeed generated (0.025 ± 0.001 μM), its level was much lower than expected, representing only 0.21% of the total amount of FFAs produced (Figure 2B).

Quantifying FFAs Following Secretagogue Stimulation in Bovine Chromaffin Cells

As cortical neurons produce very little AA, we performed the same experiment on bovine chromaffin cells (neurosecretory cells), which have been widely used to assess the effect of AA on exocytosis. Nineteen selected FFAs were identified, and most of these increased in response to stimulation (Figure 3A). Our results revealed similar findings to those found in rat cortical neurons following depolarization. Stearic, palmitic, myristic, and arachidic acids represented 84% of the generated FFAs that were detected following stimulation (Figure 3B). Importantly a small, albeit significant, increase in AA was

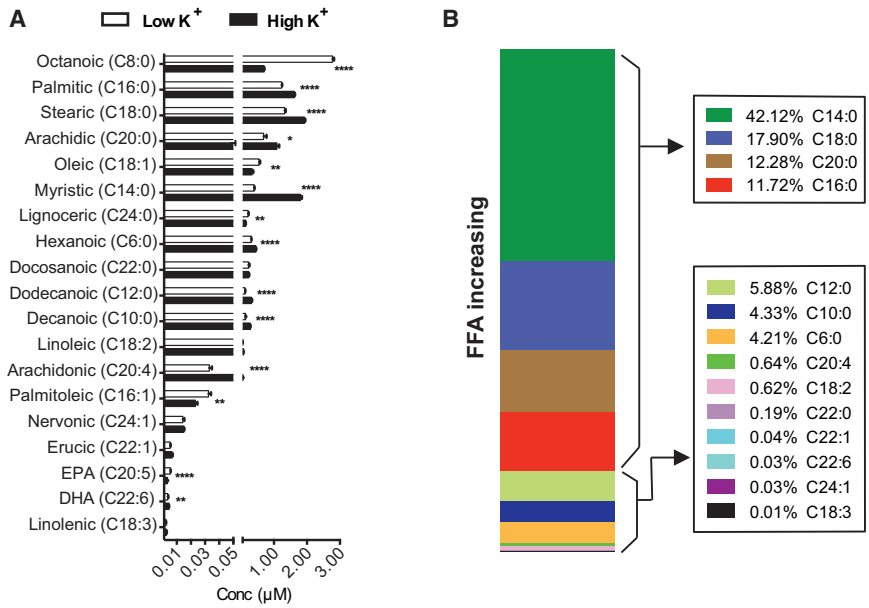

Figure 3. Quantification of FFA Changes in Neurosecretory Cells by FFAST Labeling

Bovine adrenal chromaffin cells were either stimulated for 15 min by depolarization or left unstimulated. Cells were then collected, lipids extracted, and FFAs derivatized.

(A) Changes in saturated and unsaturated FFAs elicited by stimulation as indicated.

(B) Stacked bar-graph representation of the FFAs increasing in concentration upon stimulation. The difference in concentration between unstimulated and stimulated was calculated and expressed as percentage and stacked from the highest to the lowest. Note that the main FFAs produced in response to stimulation are saturated (stearic, palmitic, myristic, and arachidic acids) and constitute 84.5% of the total amount of FFAs generated.

Data are represented as mean ± SEM; *$p < 0.05$; **$p < 0.01$; ****$p < 0.0001$, two-tailed Student's *t* test.

detected (0.57 ± 0.04 μM, representing 0.64% of the total amount of FFAs produced). The comparison of FFA changes elicited by stimulation between neurons and chromaffin cells highlights a high level of similarities in the amount of saturated and unsaturated FFAs generated.

Quantifying Changes in FFAs from Chromaffin Granules Elicited by Cytosol and Free Ca^{2+}

As chromaffin cells are filled with Chromaffin granules (CG) encompassing a large proportion of the membrane phospholipids, we wondered whether these organelles had the ability to generate FFAs and whether the addition of cytosol (Cyt) and Ca^{2+} could affect such production. We tested whether the nanomolar detection limit of our method was sensitive enough to detect absolute changes in FFAs in a subcellular fraction.

Chromaffin granules were prepared and incubated in the presence or absence of cytosol and calcium (Tomatis et al., 2013). FFAs were extracted and derivatized with FFAST-124, -127, -138, and -143. Samples were pooled and analyzed simultaneously (Figure S4) with a fixed amount of FFA standards derivatized with FFAST-152 added as internal standards.

Almost all the FFAs detected were significantly increased when chromaffin granules were incubated with cytosol, except eicosapentaenoic and octanoic acid, which showed no change in their concentrations (Figure 4A). Consistent with the previous results obtained with both chromaffin cells and neurons, the majority of the FFAs generated from chromaffin granules exposed to cytosol were saturated, including stearic and palmitic acid (Figures 4A and 4B). Importantly, we could only detect traces of FFAs in the cytosol (Figure 4A). This suggests that the cytosol contains most of the phospholipase enzymatic activity required to generate these FFAs from granules. Notably, other saturated FFAs were specifically increased from granules incubated in cytosol, such as docosanoic acid (11.6 ± 2.8 μM representing 14.5% of the total amount of FFAs generated) and lignoceric acid (representing 22.3%; Figures 4A and 4B). The difference in FFAs generated on chromaffin granules when compared with the whole cells could stem from slightly different phospholipid substrate content that resides in granules and plasma membrane. Alternatively, recruitment of slightly different phospholipases from the cytosol or some difference in substrate specificity could also account for these differences.

Interestingly, we found a very similar amount of AA generated in chromaffin granules exposed to cytosol (0.79 ± 0.07 μM; Figure 4A) compared with stimulated chromaffin cells (0.57 ± 0.04 μM; Figure 3A). However, this only represents 0.96% of the total amount of FFAs generated from the granules as opposed to 11.7% in stimulated whole cells. This suggests that granules themselves are capable of producing a significant amount of AA matching that of the plasma membrane. However, the rather large generation of saturated FFAs from granules overshadows that of AA (Figure 3).

Surprisingly, most of the FFA levels dropped when chromaffin granules and cytosol were co-incubated with free Ca^{2+} except eicosapentaenoic acid and AA (Figure 4B). Another interesting point is that Ca^{2+} significantly reduced the levels of saturated FFAs, suggesting that their production could be Ca^{2+} dependent. Alternatively, they could still be produced by addition of cytosol, but not in a free state. One possibility is that they bind to proteins in a Ca^{2+}-dependent manner, which would hamper detection as FFAs. Future work will be needed to decipher these two possibilities.

DISCUSSION

Here, we report the development of an unbiased multiplex assay for quantification of FFAs for four or more biological conditions. By taking advantage of the reactive nitrogen group of hydroxymethylpyridine, we were able to incorporate isotopic tags of varying chain lengths, and thus modulate the mass of tagged FFAs and their fragment ions (Table S1). This iTRAQ-like method

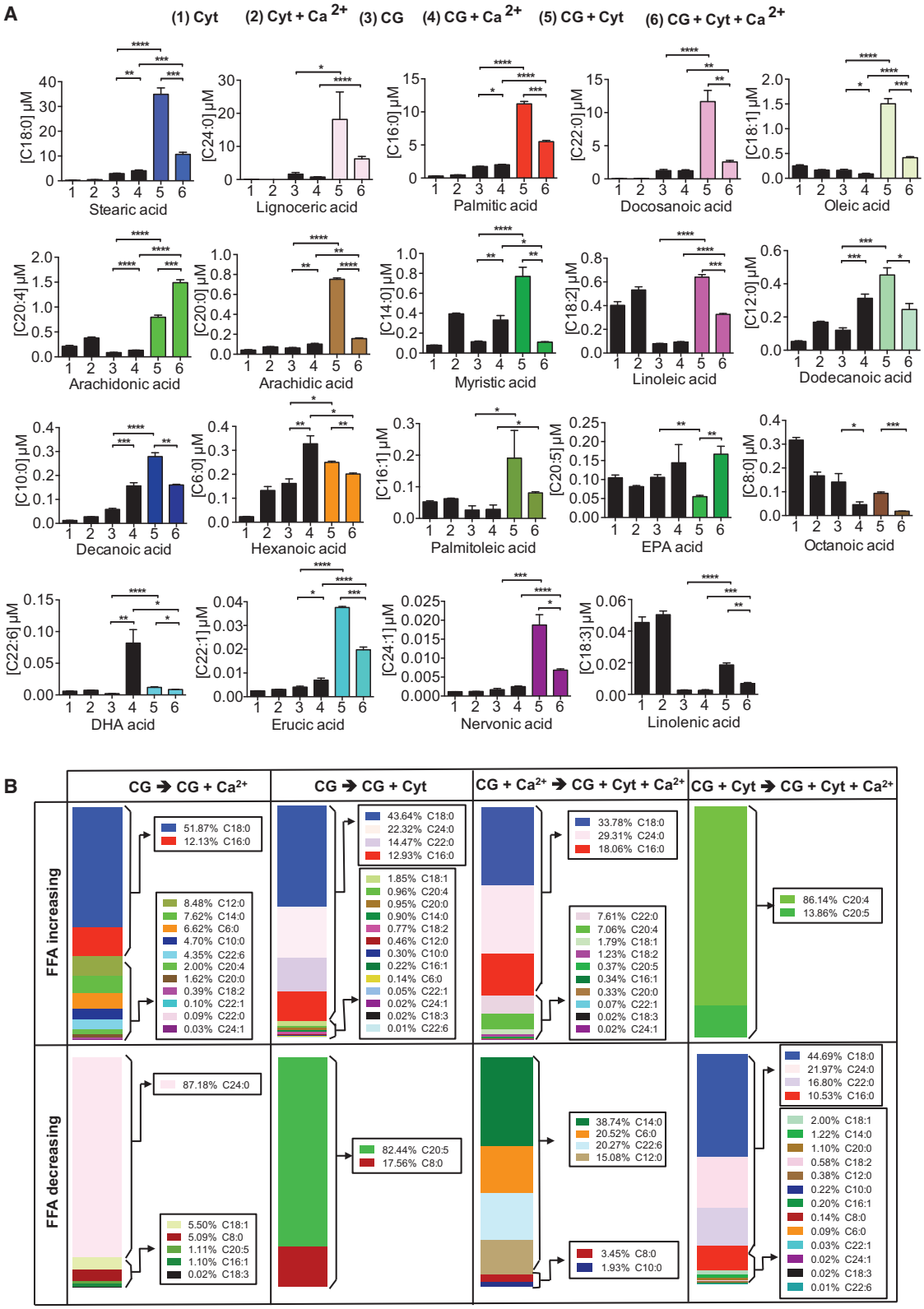

Figure 4. Quantification of FFA Changes in Chromaffin Granules of Adrenal Chromaffin Cells by FFAST Labeling

Chromaffin granules, CG (100 µg) and cytosol, Cyt (1,000 µg) freshly purified from bovine adrenal medullas were incubated in the presence or the absence of Cyt and Ca^{2+} for 30 min followed by lipid extraction and derivatization, as described in the Experimental Procedures.

(legend continued on next page)

allowed us to uncover widespread changes in FFA composition in both neurons and neurosecretory cells. The nanomolar sensitivity of the method allowed us to measure changes in FFAs from subcellular fractions, and to discover that cytosol is key to the generation of saturated FFAs from chromaffin granules, an effect that is inhibited by Ca^{2+}.

We report a simple and rapid one-step quantitative labeling reaction that can be carried out under mild conditions with high specificity, and improved analytical throughput and accuracy. An important aspect of this method is that every individual analyte is compared with its own reference internal standard, which provides a convenient means for measuring both absolute and relative levels of FFAs. This experimental methodology could therefore be useful for large clinical studies, as longer isotopically tagged side chains could be incorporated. Moreover, inclusion of carbon stable isotopes is also possible, widening the multiplexing power of this method.

One important aspect of our results is the finding that stimulation by depolarization promotes a major increase in 11–12 FFAs in both chromaffin cells and cortical neurons. Surprisingly, mostly identical FFAs increased in both systems. Their relative increase was also consistent, suggesting a common underlying coding mechanism involving specific phospholipases. The fact that so many FFAs are increased upon stimulation is interesting, particularly bearing in mind that combinations of specific FFAs and lysophospholipids have been shown to promote neurotransmitter secretion at the neuromuscular junction (Rigoni et al., 2005). Another unexpected finding was that the most abundant FFAs generated were saturated, casting strong doubt on the involvement of PLA2 activity and suggesting that the combined action of PLD1 and PLA1 (Higgs and Glomset, 1996) might primarily be involved. Indeed, finding mostly saturated FFAs being generated by stimulation was unexpected, as most of the current literature on neuroexocytosis has focused on an involvement of PLD1 and PLA2 (Frye and Holz, 1984; Latham et al., 2007; Morgan and Burgoyne, 1990; Rickman and Davletov, 2005). Clearly more work is needed to reassess the key steps leading to neuroexocytosis and establish a potential role for PLA1, capable of cleaving the *sn-1* position of phospholipids (Inloes et al., 2014). Interestingly, mutations in phosphatidic acid-PLA1 have recently been linked to cases of congenital paraplegia, and a potential effect on synaptic secretion has been suggested (Gonzalez et al., 2013). Finally, the increase in AA detected was relatively minor in both chromaffin and cortical neurons in the low-micromolar range. However, these smaller changes might be functionally relevant (Frye and Holz, 1984; Latham et al., 2007; Morgan and Burgoyne, 1990; Rickman and Davletov, 2005).

The high sensitivity of the FFAST method allowed us to detect minute changes in subcellular fractions such as chromaffin granules. To the best of our knowledge, this is the first report of comprehensive FFA profiling done in a subcellular fraction. Such sensitivity will enable future projects examining the role of FFA in other important subcellular fractions such as the Golgi apparatus or the ER, where palmitoylation can occur (Charollais and Van Der Goot, 2009). Importantly, adding cytosol to chromaffin granules strongly increases the amount of FFA produced. This is not surprising, as most phospholipases are located in the cytosol. Notably, the nature of the FFAs elicited by the addition of cytosol was practically identical to that found in the whole-cell experiments using either neurons or chromaffin cells. This suggests that the changes in FFAs produced in neurons and neurosecretory cells are likely to be generated at the level of a subpopulation of these granules. Another interesting aspect is the reduction in FFAs detected in many species in the presence of free Ca^{2+}, suggesting that Ca^{2+} can trigger the recruitment of selective species of FFA to specific proteins or block phospholipase activity. Future work manipulating the levels and/or activity of various phospholipases will be needed to understand the functional significance of this Ca^{2+} inhibition.

Our method is therefore a useful addition to the current arsenal of assays that are capable of providing an unbiased and holistic profiling of changes occurring in biological membranes during physiological or pathological manipulations.

SIGNIFICANCE

We have developed and implemented a holistic and unbiased iTRAQ-like multiplex method that utilizes stable isotope tagging with differential labeling of the FFA carboxyl group to detect FFA changes with nanomolar sensitivity. Taking advantage of the sensitivity of this technique, we have profiled the changes in FFAs taking place during neuroexocytosis from both cultured neurons and neurosecretory cells by providing direct comparisons of relative and absolute measurements of four or more biological conditions, carried out in one MS analysis. Using this novel method, we have unraveled an unsuspectedly wide range of saturated FFAs generated during neuroexocytosis. We also detected minute changes in saturated FFAs elicited from subcellular chromaffin vesicle fractions. These results have profound implications for our understanding of the molecular mechanism underpinning neuroexocytosis. The fact that saturated FFAs are mainly generated in stimulated neurons and neurosecretory cells is highly surprising, as previous reports pointed to PLA2 activity being activated during exocytosis, leading to the release of unsaturated FFAs. Our results show that PLA1 is likely to be activated, leading to the generation of saturated FFAs through cleavage at the *sn*-1 position. The results generated using this innovative method provide a paradigm shift in our understanding of the mechanism of exocytosis. Our method is likely also to help unravel key changes in FFAs generated during specific paradigms including brain development and plasticity, inflammation, infection, cancer, and many others, and promises to be useful for both applied and basic biomedicine.

(A) Changes in saturated and unsaturated FFAs elicited upon Ca^{2+} and cytosol addition.
(B) Stacked bar graphs (from left to right) representing the FFAs that increased (top) and decreased (bottom) in concentration upon stimulation. The difference in concentration between unstimulated and stimulated was calculated and expressed as a percentage, and stacked from the highest to the lowest.
Data are represented as mean ± SEM; *$p < 0.05$; **$p < 0.01$; ***$p < 0.001$; ****$p < 0.0001$, two-tailed Student's *t*-test. See also Figures S3 and S4.

EXPERIMENTAL PROCEDURES

Materials

Analytical standards were obtained from Sigma-Aldrich for saturated fatty acids (Cat. No. EC10A-1KT, containing arachidic acid [C20:0], behenic acid [C22:0], decanoic acid [C10:0], dodecanoic acid [C12:0], hexanoic acid [C6:0], lignoceric acid [C24:0], myristic acid [C14:0], octanoic acid [C8:0], palmitic acid [C16:0], stearic acid [C18:0]), unsaturated fatty acids (Cat. No. UN10-1KT, containing arachidonic acid [C20:4], *cis*-4,7,10,13,16,19-docosahexaenoic acid [C22:6], erucic acid [C22:1], linoleic acid [C18:2], linolenic acid [C18:3], nervonic acid [C24:1], oleic acid [C18:1], palmitoleic acid [C16:1]), *cis*-5,8,11,14,17-eicosapentaenoic acid [C20:5] (Cat. No. 44864), and stearic-d_{35} acid [C18:0-d_{35}] (Cat. No. 448249). All chemicals, including 1,1-carbonydiimidiazole, triethylamine, iodomethane, iodomethane-d_3, iodoethane, iodoethane-d_5, iodopropane, analytical-grade formic acid, acetonitrile (ultra-gradient grade), and all other reagents, unless specified, were purchased from Sigma-Aldrich. Ultra-pure water was used for all the preparations. All cell-culture reagents were from Life Technologies unless specified. All lipid extractions used 2-ml polypropylene LoBind safe-lock tubes (Eppendorf).

Synthesis of Isotopic Coded Differential Tags: FFAST-124, FFAST-127, FFAST-138, FFAST-143, and FFAST-152

All the isotopic coded differential tags were prepared in a similar fashion (Figure 1A) starting from commercially available $CH_3I/CD_3I/C_2H_5I/C_2D_5I/C_3H_7I$ and 3-hydroxymethylpyridine. The synthesis of FFAST derivatives was according to procedures described by Yang et al. (2007) and Koulman et al. (2009) with modifications. In brief, 100 mg of 3-hydroxymethylpyridine was added to 200 mg of iodomethane, iodomethane-d_3, iodoethane, iodoethane-d_5, and iodopropane respectively. The solution was heated in a Discover Benchmate microwave reactor (CEM Corporation) at 90°C for 90 min (microwave power 1–300 W) under nitrogen atmosphere. The resulting solid was washed with diethyl ether and subsequently dried. The purity of all the derivatives was determined to be >95% by ^{1}H NMR.

Cell Cultures

Chromaffin cells were prepared from bovine adrenal glands as described previously (Meunier et al., 2002, 2005), and cultured in DMEM supplemented with 10% serum supreme, 50 μg/ml gentamicin, 10 mM HEPES, and 2.5 μg/ml fungizone at 37°C in 5% CO_2 for at least 24 hr before experimentation. Chromaffin granules and cytosol purified from bovine adrenal medullas were fractionated as previously described (Meunier et al., 2005; Tomatis et al., 2013; Wen et al., 2011). Cortical neurons were isolated from embryonic-day-18 Sprague-Dawley rat embryos and digested with 0.25% trypsin/EDTA for 20 min at 37°C, followed by trituration with pipettes in plating medium (DMEM with 10% fetal bovine serum and 10% F12 supplements). Dissociated neurons were seeded onto dishes coated with poly-D-lysine (0.05 mg/ml) at a density of 5 × 10^5/cm^2. Culturing for 24 hr, the plating medium was replaced with neuronal culture medium (neurobasal medium containing 1% GlutaMAX and 2% B27 supplements), while cultures were maintained for 21 days in vitro with a change of medium twice a week. The cells were cultured for at least 3 weeks before experimentation. The Animal Ethics Committee at the University of Queensland approved all the experimental procedures. The animal ethics permit number for the experiments is QBI/313/13/NHMRC.

Fatty Acid Extraction

Chromaffin Cells and Cortical Neurons

Bovine chromaffin cells that had been cultured for 24 hr and 3-week-old cortical cultured neurons were washed with Low K^+ buffer A (145 mM NaCl, 5 mM KCl, 1.2 mM Na_2HPO_4, 20 mM HEPES-NaOH, 2 mM $CaCl_2$, 10 mM glucose [pH 7.4]) and were treated with either Low K^+ buffer A or High K^+ buffer (90 mM NaCl, 60 mM KCl, 1.2 mM Na_2HPO_4, 20 mM HEPES-NaOH, 2 mM $CaCl_2$, 10 mM glucose [pH 7.4]) for 15 min at 37°C. Cells were collected and the FFA extraction with MTBE was performed according to Matyash et al. (2008). In brief, 200 μl of methanol was added to the cells and the tube vortexed. Then 1 ml of MTBE was added and the mixture was incubated for 1 hr at room temperature in a shaker. The addition of 1.25 ml of ultra-pure-grade water induced phase separation. The mixture was further incubated for 10 min at room temperature and the sample was centrifuged at 1,000 × *g* for 10 min. The upper organic phase was collected, and the lower phase was re-extracted with 2 ml of solvent mixture containing MTBE/water/methanol (10:2.3:3 v/v/v). The upper organic phase was collected, combined with the first organic extract, and dried in a vacuum concentrator (Genevac Ltd). The extracted FFAs were re-dissolved in acetonitrile (100 μl).

Cytosol and Secretory Granule Purification from Bovine Adrenal Medulla

Bovine adrenal medullas were fractionated as previously described (Simon et al., 1988; Tomatis et al., 2013; Wen et al., 2011). In brief, isolated bovine adrenal medullas were homogenized in 0.32 M sucrose in 10 mM Tris and 1 mM EGTA (pH 7.4). The homogenate was subjected to 2 × 15-min centrifugation at 800 × g_{av}. The supernatant was re-centrifuged for 20 min at 12,000 × g_{av}, after which the pellet was resuspended in 0.32 M sucrose in 10 mM Tris and 1 mM EGTA (pH 7.4) and loaded on a linear sucrose gradient (34%–68%) before 1 hr centrifugation at 100,000 × g_{av}. 12 × 1-ml fractions were collected from the top of the gradient. The supernatant from the 12,000 × g_{av} spin (12KSN) was further centrifuged for 1 hr at 100,000 × g_{av} and the resulting supernatant was collected (100KSN). For the cytosol preparation, the 100KSN fraction was dialyzed overnight at 4°C in potassium glutamate buffer (KGEP buffer; 139 mM potassium glutamate, 5 mM glucose, 5 mM EGTA, and 20 mM PIPES-NaOH [pH 6.8]) containing 2 mM of free $MgCl_2$, 2 mM ATP, and 0 or 100 μM free Ca^{2+}.

Calcium- and Cytosol-Dependent Change in FFAs from Isolated Chromaffin Secretory Granules

Secretory granules and cytosol purification was performed as previously described (Tomatis et al., 2013; Wen et al., 2011). In brief, purified chromaffin granules (100 μg) were incubated in the presence or absence of purified cytosol (1 mg) for 30 min at 37°C in KGEP buffer containing either 0 or 100 mM Ca^{2+}. Reactions were stopped by adding 750 μl of ice-cold KGEP buffers. Chromaffin granules were then ultracentrifuged, twice for 45 min at 50,000 rpm and 4°C, with a wash step in between using KGEP buffers. The final pellet was resuspended with methanol and used for FFA extraction as described above.

Derivatization of FFAs

The derivatization of FFAs was performed according to a procedure described previously (Koulman et al., 2009) with modifications. In brief, 100 μl of FFA solutions (standards or cell/tissue extracts in acetonitrile) were mixed with 50 μl of 1,1-carbonyldiimidiazole (1 mg/ml in acetonitrile), and incubated for 2 min at room temperature. For each biological condition being tested (up to four conditions), 50 μl of either FFAST-124, FFAST-127, FFAST-138, or FFAST-143 (50 mg/ml in acetonitrile + 5% triethylamine) was added. After mixing for 2 min, the mixtures were heated in a water bath at 50°C for 20 min. Finally the isotopically labeled samples from each condition were mixed together in a ratio of 1:1 v/v (2 conditions, final volume 400 μl) or 1:1:1:1 v/v/v/v (4 conditions, final volume 800 μl), respectively. The samples were dried in a vacuum concentrator (Genevac Ltd), and were re-dissolved in 200 μl of an internal standard solution (2.5 μM in acetonitrile) that was prepared in a preliminary step by derivatization of the 19 FFA standards with the FFAST-152 label, as above. FFA standards were prepared from stock solutions (0.20 mg/ml) in acetone/acetonitrile (2:1 v/v). Calibrators (0.3 to 300 nM) and quality controls (1, 6 and 15 nM) were made in acetonitrile from serial dilutions of the standards. The FFA calibrators were activated using 1,1-carbonyldiimidiazole and derivatized with the FFAST labels as above, then evaporated to dryness and reconstituted using non-derivatized blank cell extracts in acetonitrile (200 μl). Samples and standards were stored at −20°C before being subjected to analysis.

LC/Electrospray Ionization-MS/MS Analysis

The LC-MS/MS analysis was performed on a 5500QTRAP tandem mass spectrometer with an electrospray ionization TurboIonSpray source (AB Sciex), connected to a Shimadzu Nexera UHPLC equipped with an XB-C18 Kinetex column, 50 × 2.1 mm, 1.7 μm (Phenomenex). Instrument control and data acquisition were performed using Analyst 1.5.2 software. The instrument

was operated in the positive ion mode under multiple reaction-monitoring conditions. The Turbospray temperature was set to 400°C, the curtain gas flow to 30 psi, and the ion spray voltage to 4,500 V. The collision energy, declustering potential, and collision cell exit potential were optimized and set to 55, 100, and 13 V, respectively. The mobile phase system consisted of solvent A (water/acetonitrile [99:1 v/v] + 0.1% formic acid) and solvent B (acetonitrile/water [90:10 v/v] + 0.1% formic acid), using a flow rate of 400 μl/min. After equilibration with 40% B, the gradient elution used was 40%–62% B (0.8 min), 62% B (1 min), 62%–100% B (1.2 min), 100% B (1 min), then 40% B (2 min), total run time 6 min. The first 0.5 min of the LC run was switched to waste to remove the excess underivatized FFAST tags. The chromatograms were acquired between 0.5 and 6 min (Figures S1 and S2). The column was preconditioned with 40% (B) for 30 min before a batch analysis. Samples were reconstituted from 100 μl of mobile phase A, and 5 μl was injected onto the column using a peak-focusing injection sequence (pretreatment program using 5 μl of sample + 45 μl of water in a 50-μl loop).

SUPPLEMENTAL INFORMATION

Supplemental Information includes five tables and four figures and can be found with this article online at http://dx.doi.org/10.1016/j.chembiol.2015.09.010.

AUTHOR CONTRIBUTIONS

V.K.N., D.K., and F.A.M. conceived the study and designed the research. V.K.N. developed methods, performed research, and analyzed the data. V.K.N. and V.M.T. prepared chromaffin granules and cytosol and performed chromaffin granules experiments. T.W. performed cortical neuron cultures. V.K.N., D.K., and F.A.M. were involved in all the discussions and wrote the manuscript. D.K. and F.A.M supervised the study.

ACKNOWLEDGMENTS

The authors would like to thank Rachel Gormal for helping in the preparation of adrenal chromaffin cells. This work was supported by a National Health and Medical Research Council (NHMRC) project grant (APP1058769). F.A.M. is an NHMRC Senior Research Fellow (APP1060075).

Received: July 8, 2015
Revised: September 2, 2015
Accepted: September 24, 2015
Published: October 22, 2015

REFERENCES

Carta, M., Lanore, F., Rebola, N., Szabo, Z., Da Silva, S.V., Lourenco, J., Verraes, A., Nadler, A., Schultz, C., Blanchet, C., et al. (2014). Membrane lipids tune synaptic transmission by direct modulation of presynaptic potassium channels. Neuron *81*, 787–799.

Charollais, J., and Van Der Goot, F.G. (2009). Palmitoylation of membrane proteins (review). Mol. Membr. Biol. *26*, 55–66.

Darios, F., Connell, E., and Davletov, B. (2007). Phospholipases and fatty acid signalling in exocytosis. J. Phys. *585*, 699–704.

Frye, R.A., and Holz, R.W. (1984). The relationship between arachidonic acid release and catecholamine secretion from cultured bovine adrenal chromaffin cells. J. Neurochem. *43*, 146–150.

Gonzalez, M., Nampoothiri, S., Kornblum, C., Oteyza, A.C., Walter, J., Konidari, I., Hulme, W., Speziani, F., Schols, L., Zuchner, S., et al. (2013). Mutations in phospholipase DDHD2 cause autosomal recessive hereditary spastic paraplegia (SPG54). Eur. J. Hum. Gen. *21*, 1214–1218.

Hellmuth, C., Weber, M., Koletzko, B., and Peissner, W. (2012). Nonesterified fatty acid determination for functional lipidomics: comprehensive ultra-high performance liquid chromatography-tandem mass spectrometry quantitation, qualification, and parameter prediction. Anal. Chem. *84*, 1483–1490.

Higgs, H.N., and Glomset, J.A. (1996). Purification and properties of a phosphatidic acid-preferring phospholipase A1 from bovine testis. Examination of the molecular basis of its activation. J. Biol. Chem. *271*, 10874–10883.

Inloes, J.M., Hsu, K., Dix, M.M., Vaider, A., Masuda, K., Takei, T., Wood, M.R., and Cravatt, B.F. (2014). The hereditary spastic paraplegia-related enzyme DDHD2 is a principal brain triglyceride lipase. Proc. Natl. Acad. Sci. USA *111*, 14924–14929.

Johnson, D.W. (2005). Contemporary clinical usage of LC/MS: analysis of biologically important carboxylic acids. Clin. Biochem. *38*, 351–361.

Johnson, D.W., and Trinh, M.U. (2003). Analysis of isomeric long-chain hydroxy fatty acids by tandem mass spectrometry: application to the diagnosis of long-chain 3-hydroxyacyl CoA dehydrogenase deficiency. Rapid Commun. Mass Spectrom. *17*, 171–175.

Kanawati, B., and Schmitt-Kopplin, P. (2010). Exploring rearrangements along the fragmentation of glutaric acid negative ion: a combined experimental and theoretical study. Rapid Commun. Mass Spectrom. *24*, 1198–1206.

Kihara, Y., Maceyka, M., Spiegel, S., and Chun, J. (2014). Lysophospholipid receptor nomenclature review: IUPHAR review 8. Br. J. Pharmacol. *171*, 3575–3594.

Koulman, A., Petras, D., Narayana, V.K., Wang, L., and Volmer, D.A. (2009). Comparative high-speed profiling of carboxylic acid metabolite levels by differential isotope-coded MALDI mass spectrometry. Anal. Chem. *81*, 7544–7551.

Lamos, S.M., Shortreed, M.R., Frey, B.L., Belshaw, P.J., and Smith, L.M. (2007). Relative quantification of carboxylic acid metabolites by liquid chromatography-mass spectrometry using isotopic variants of cholamine. Anal. Chem. *79*, 5143–5149.

Latham, C.F., Osborne, S.L., Cryle, M.J., and Meunier, F.A. (2007). Arachidonic acid potentiates exocytosis and allows neuronal SNARE complex to interact with Munc18a. J. Neurochem. *100*, 1543–1554.

Leng, J., Wang, H., Zhang, L., Zhang, J., Wang, H., and Guo, Y. (2013). A highly sensitive isotope-coded derivatization method and its application for the mass spectrometric analysis of analytes containing the carboxyl group. Anal. Chim. Acta *758*, 114–121.

Li, X., and Franke, A.A. (2011). Improved LC-MS method for the determination of fatty acids in red blood cells by LC-orbitrap MS. Anal. Chem. *83*, 3192–3198.

Matyash, V., Liebisch, G., Kurzchalia, T.V., Shevchenko, A., and Schwudke, D. (2008). Lipid extraction by methyl-tert-butyl ether for high-throughput lipidomics. J. Lipid Res. *49*, 1137–1146.

Meunier, F.A., Feng, Z.P., Molgo, J., Zamponi, G.W., and Schiavo, G. (2002). Glycerotoxin from *Glycera convoluta* stimulates neurosecretion by up-regulating N-type Ca^{2+} channel activity. EMBO J. *21*, 6733–6743.

Meunier, F.A., Osborne, S.L., Hammond, G.R., Cooke, F.T., Parker, P.J., Domin, J., and Schiavo, G. (2005). Phosphatidylinositol 3-kinase C2alpha is essential for ATP-dependent priming of neurosecretory granule exocytosis. Mol. Biol. Cell *16*, 4841–4851.

Moldovan, Z., Jover, E., and Bayona, J.M. (2002). Gas chromatographic and mass spectrometric methods for the characterisation of long-chain fatty acids—application to wool wax extracts. Anal. Chim. Acta *465*, 359–378.

Morgan, A., and Burgoyne, R.D. (1990). Relationship between arachidonic acid release and Ca2(+)-dependent exocytosis in digitonin-permeabilized bovine adrenal chromaffin cells. Biochem. J. *271*, 571–574.

Raghupathy, R., Anilkumar, A.A., Polley, A., Singh, P.P., Yadav, M., Johnson, C., Suryawanshi, S., Saikam, V., Sawant, S.D., Panda, A., et al. (2015). Transbilayer lipid interactions mediate nanoclustering of lipid-anchored proteins. Cell *161*, 581–594.

Ray, P., Berman, J.D., Middleton, W., and Brendle, J. (1993). Botulinum toxin inhibits arachidonic acid release associated with acetylcholine release from PC12 cells. J. Biol. Chem. *268*, 11057–11064.

Rickman, C., and Davletov, B. (2005). Arachidonic acid allows SNARE complex formation in the presence of Munc18. Chem. Biol. *12*, 545–553.

Rigoni, M., Caccin, P., Gschmeissner, S., Koster, G., Postle, A.D., Rossetto, O., Schiavo, G., and Montecucco, C. (2005). Equivalent effects of snake PLA2 neurotoxins and lysophospholipid-fatty acid mixtures. Science *310*, 1678–1680.

Seppanen-Laakso, T., Laakso, I., and Hiltunen, R. (2002). Analysis of fatty acids by gas chromatography, and its relevance to research on health and nutrition. Anal. Chim. Acta *465*, 39–62.

Shimizu, T. (2009). Lipid mediators in health and disease: enzymes and receptors as therapeutic targets for the regulation of immunity and inflammation. Ann. Rev. Pharmacol. Toxicol. *49*, 123–150.

Simon, J.P., Bader, M.F., and Aunis, D. (1988). Secretion from chromaffin cells is controlled by chromogranin A-derived peptides. Proc. Natl. Acad. Sci. USA *85*, 1712–1716.

Tomatis, V.M., Papadopulos, A., Malintan, N.T., Martin, S., Wallis, T., Gormal, R.S., Kendrick-Jones, J., Buss, F., and Meunier, F.A. (2013). Myosin VI small insert isoform maintains exocytosis by tethering secretory granules to the cortical actin. Cell Biol. *200*, 301–320.

U.S. Department of Health and Human Services, Food and Drug Administration, Center for Drug Evaluation and Research (CDER), and Center for Veterinary Medicine (CVM). (2001). Guidance for Industry, Bioanalytical Method Validation (FDA).

U.S. Department of Health and Human Services, Food and Drug Administration, Center for Drug Evaluation and Research (CDER), and Center for Veterinary Medicine (CVM). (2013). Guidance for Industry, Bioanalytical Method Validation, Draft Guidance, (FDA).

Wen, P.J., Osborne, S.L., Zanin, M., Low, P.C., Wang, H.T., Schoenwaelder, S.M., Jackson, S.P., Wedlich-Soldner, R., Vanhaesebroeck, B., Keating, D.J., et al. (2011). Phosphatidylinositol(4,5)bisphosphate coordinates actin-mediated mobilization and translocation of secretory vesicles to the plasma membrane of chromaffin cells. Nat. Commun. *2*, 491.

Wiese, S., Reidegeld, K.A., Meyer, H.E., and Warscheid, B. (2007). Protein labeling by iTRAQ: a new tool for quantitative mass spectrometry in proteome research. Proteomics *7*, 340–350.

Williams, J.H., Errington, M.L., Lynch, M.A., and Bliss, T.V. (1989). Arachidonic acid induces a long-term activity-dependent enhancement of synaptic transmission in the hippocampus. Nature *341*, 739–742.

Yang, W.C., Adamec, J., and Regnier, F.E. (2007). Enhancement of the LC/MS analysis of fatty acids through derivatization and stable isotope coding. Anal. Chem. *79*, 5150–5157.